J. Coat. Technol. Res.
https://doi.org/10.1007/s11998-019-00312-4

Exploration of high corrosion resistance property of less hazardous pyrazolidine-based benzoxazines in comparison with bisphenol-F derivatives

M. Manoj, A. Kumaravel, R. Mangalam, P. Prabunathan, A. Hariharan, M. Alagar

Abstract The present work describes the design of nontoxic pyrazolidine bisphenol (PYBP)-based hydrophobic benzoxazine (PBz) matrices, in comparison with that of bisphenol-F-based benzoxazines, and investigates their efficiency toward corrosion protection on mild steel surfaces. The preliminary in vitro toxicity assay studies infer the nontoxic nature of PYBP. Data obtained from thermal and surface studies indicate that the PYBP-based PBzs possess higher thermal stability than those of bisphenol-F benzoxazines. Observations from SEM images suggest that the inherent hydrophobic nature was due to the formation of rough surfaces. The corrosion studies of the specimens were carried out using open-circuit potential, electrochemical impedance spectroscopy, and potentiodynamic polarization. Among the mild steel specimens, coated with different benzoxazines, the poly(PYBP-oda)-coated specimen was found to be less aggressive toward corrosion showing 90% efficiency and charge transfer resistance (R_{ct}) of 381 kΩ cm^2. Thus, data obtained from different studies suggest that the PYBP-based benzoxazines can be used as a better coating material for steel and steel products against corrosion.

Keywords Pyrazolidine bisphenol, Nontoxic behavior, Polybenzoxazine, Electrochemical impedance, Corrosion resistance, Corrosion efficiency

Introduction

Mild steel (MS) and stainless steel (SS) have unique mechanical properties, and therefore, they were extensively used as structural materials for many industrial, construction, and marine applications.[1,2] However, MS is extremely susceptible to metallic corrosion which leads to substantial waste of natural resources and incurs heavy expenditures to protect it.[3] SS, on the other hand, even though it is passivated and possesses resistance against corrosion, is also not able to meet the requirements for corrosion-resistant behavior under peculiar conditions, and thus, wider applications of SS are also limited. During corrosion, the physicochemical properties of the steel are altered which leads to partial/complete damage of the steel structure and eventually ruining the whole purpose of its application. In this overview, an effective anticorrosive coating material is being developed to avoid/control the metallic corrosion.[4–7] The application of polymer-based protective coatings over the metal surfaces is an effective method and is a universally applied strategy to inhibit the corrosion process.[8–11] The polymer coating also provides the desired aesthetic properties which play a vital role in the protection of metals from radiation, moisture, chemical damage, and biological corrosion.[12] The polymer coating is considered to prevent the contact of water or ions to the metallic surface by generating a physical barrier and thus significantly reducing the corrosion currents due

Electronic supplementary material The online version of this article (https://doi.org/10.1007/s11998-019-00312-4) contains supplementary material, which is available to authorized users.

M. Manoj, P. Prabunathan, A. Hariharan, M. Alagar (✉)
Polymer Engineering Laboratory, PSG Institute of Technology and Applied Research, Neelambur, Coimbatore 641 062, India
e-mail: mkalagar@yahoo.com

A. Kumaravel
Department of Chemistry, PSG Institute of Technology and Applied Research, Neelambur, Coimbatore 641 062, India

R. Mangalam
Department of Physics, PSG Institute of Technology and Applied Research, Neelambur, Coimbatore 641 062, India

Published online: 03 February 2020

to the decreased anodic reaction.[13] Corrosion-resistant coatings based on organic resins (such as epoxy resins, polysiloxane resins, and polyurethane resins) have been employed to protect steel surfaces from corrosive environments by providing a firm and protective impervious film to prevent the diffusion of the corrosive species (ionic transport) and electrical conduction onto the metal surface.[14,15] Usually, the organic compounds that are rich in heteroatoms (such as nitrogen, sulfur, and oxygen) can act as efficient corrosion inhibitors.[16,17] Similarly, the crosslinking density and hydrophobic nature of polymer coatings also facilitate the protection of steel surfaces from corrosive electrolytes.[18–20]

In recent years, polybenzoxazines (PBz) have attracted great interest in anticorrosion coatings owing to their distinct advantages such as flexibility in molecular design, low water absorption, low flammability, low surface free energy, zero volume shrinkage upon curing, low dielectric constant, and higher glass transition temperature.[21–26] The coatings based on PBz can act as a physical barrier which can protect the surface of the metal from the corrosive environments by limiting the ionic permeability and electrical conduction. Molecular design flexibility with different functional groups in the PBz skeleton is the main advantage of this polymer, and it can be synthesized using phenol, amine, and formaldehyde as precursors.[27] For example, bisphenol-A is considered as an important precursor for the preparation of conventional PBz resin due to its easy availability, high purity, and inexpensive nature.[28] Hence, the preparation of BPA-based benzoxazine monomers exceeds 4.5 million tons every year. Owing to the same fact, the application of BPA-based PBz for corrosion resistance is a widely used strategy in the field of anticorrosive materials.[29,30] However, the genotoxicity and endocrine-disrupting activity of BPA causes serious health issues for humans.[31,32] The same issues occur when applied as an anticorrosive coating material in marine environment, which also affects the aquatic life,[33,34] and consequently BPA-based products are under scrutiny.[35] Owing to this fact, BPA is increasingly replaced by structurally similar chemicals, in particular, bisphenol-F (BPF).[36,37] Therefore, BPF-based PBzs emerge as a class of new polymer materials for various applications. However, BPF also exhibits a certain degree of toxic behavior, and hence, the development of alternative nontoxic precursor materials is warranted.[38]

On the other hand, BPA-based PBzs are being replaced with other heterocyclic PBzs. These superior classes of polymers account for their excellent mechanical performance, outstanding heat and flame retardant behavior, and improved molecular design flexibility when compared to those of conventional novolac, resole-type phenolics, and epoxy resins.[39] Apart from these, the value additions of these systems are high char yield, high glass transition temperature, and amenability for noncatalytic polymerization.[40–43] Earlier, our group has prepared heterocyclic imidazole core bisphenol and explored the potential applications of imidazole core bisphenol-based benzoxazine monomers and polyimides.[44–46] Thus, our continued interest has motivated us to introduce pyrazolidine bisphenol as a precursor to prepare novel benzoxazine monomers.

With this perspective, the present work focuses on the possible replacement of toxic BPA with newly prepared pyrazolidine bisphenol (PYBP) and less toxic BPF for the preparation of PBzs and the study of their application as anticorrosive coating materials. In this respect, the amines with inherent hydrophobic behavior such as dodecylamine (dda), octadecylamine (oda), and 4-fluoroaniline (fa)[47] were selected to synthesize corresponding benzoxazines (Schemes 1 and 2). Data obtained from different studies are discussed and reported.

Experimental

Chemicals

BPF was obtained from Anabond Limited, Chennai, India. 4-Hydroxybenzaldehyde and 4-hydroxyacetophenone were purchased from Sigma-Aldrich. Paraformaldehyde, dioxane, hydrazine hydrate, *para*-toluenesulphonic acid (PTSA), and acetic acid were obtained from Qualigens, India. Dodecylamine (dda), octadecylamine (oda), and 4-fluoroaniline (fa) were obtained from SRL, India. Anhydrous sodium sulfate, ethanol, and ethyl acetate were obtained from Loba Chemicals, India. Mild steel was procured from local vendor in Coimbatore, Tamil Nadu, India.

Synthesis of 1-(3,5-bis(4-hydroxyphenyl)-4, 5-dihydro-1H-pyrazol-1-yl)ethanone or pyrazolidine bisphenol (PYBP)

1-(3,5-Bis(4-hydroxyphenyl)-4,5-dihydro-1*H*-pyrazol-1-yl)ethanone or pyrazolidine bisphenol (PyBF) was prepared in accordance with the reported literature[48] (Scheme 1) with slight modification. To a solution of 4-hydroxybenzaldehyde (7.55 g, 0.05 mol) and 4-hydroxyacetophenone (16.5 g, 0.05 mol) in ethanol (50 mL), PTSA (1.72 g, 0.01 mol) was added and refluxed for 5 h with constant stirring (Scheme 1). After the formation of product was monitored through TLC, ethanol was removed partially, and the reaction mixture was added to crushed ice to obtain the chalcone intermediate as yellow precipitate (Yield = 82%).

In the next step (Scheme 1), the chalcone (10 g, 0.042 mol) was dissolved in acetic acid (30 mL) and hydrazine monohydrate (21 mL, 0.042 mol) was added and refluxed for 6 h. After the formation of product was monitored through TLC, the reaction mixture was cooled and added to crushed ice to obtain the product PYBP as light brown colored precipitate. The precip-

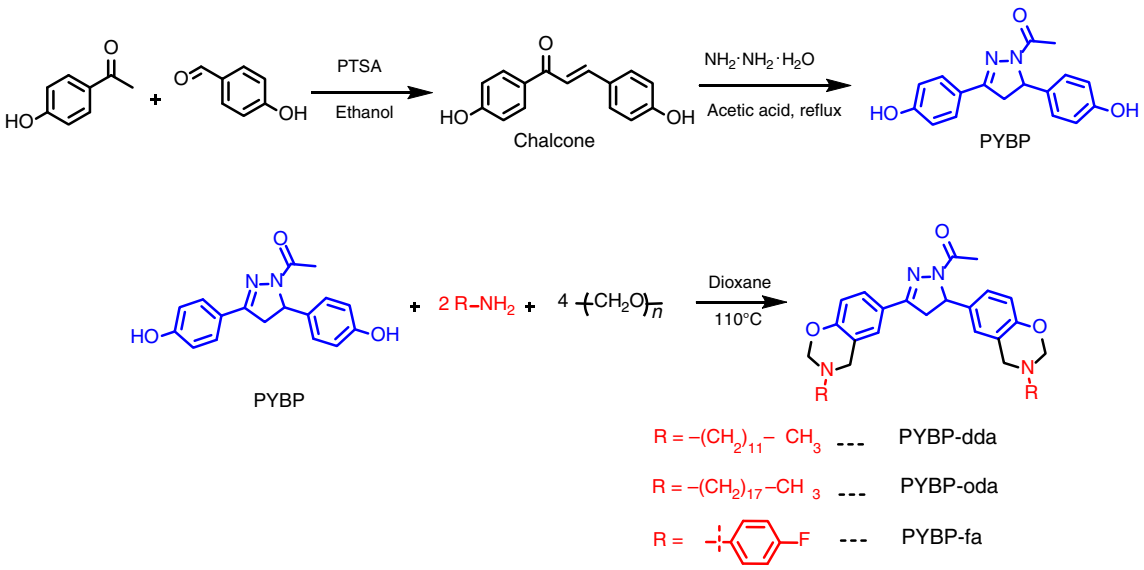

Scheme 1: Preparation of PYBF-dda, PYBF-oda, and PYBF-fa

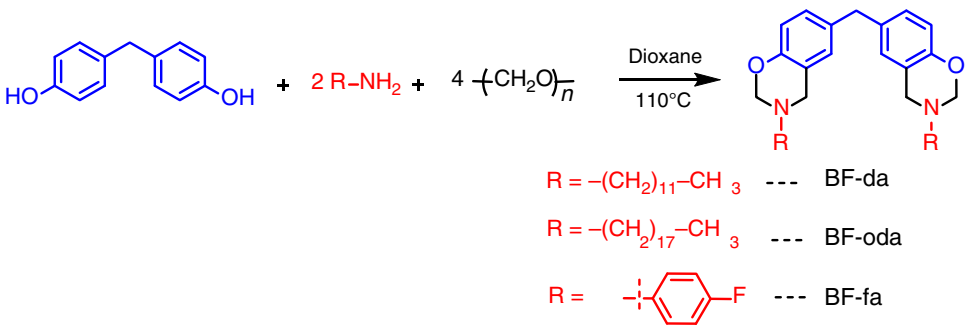

Scheme 2: Preparation of BF-dda, BF-oda, and BF-fa

itate was filtered, washed with water, and dried. The product was recrystallized using methanol (Yield = 76%). After recrystallization, the product was studied for structural confirmation using FTIR (Figure S1), ^{1}H-NMR (Figure S2), and mass spectral analysis (Figure S3). ^{1}H-NMR, (DMSO-d_6): δ 2.24 (s, 3H), 2.99–3.05 (m, 1H), 3.69–3.76 (m, 1H), 5.37–5.41 (m, 1H), 6.66–6.97 (m, 8H), 9.33 [s, 1H (OH)], 9.95 [s, 1H (OH)], ppm. MS: m/z = 296 (base peak = 295 appeared in negative mode).

Preparation of pyrazolidine-bisphenol-based benzoxazine monomer (PYBP-dda, PYBP-oda, PYBP-fa)

To prepare the benzoxazine monomer (Scheme 1), the bisphenol, PYBF (5 g, 0.17.90 mmol), respective amines [dodecylamine (dda), octadecylamine (oda), and 4-fluoroaniline (fa) 33.80 mmol], and paraformaldehyde (2.23 g, 74.35 mmol) were added separately to a round-bottom flask containing 1,4-dioxane (8 mL) and slightly warmed to 60°C to achieve homogeneity. Then the reaction temperature was raised to 110°C and stirred for 15 h. The progress of the reaction was monitored by TLC. After the formation of the product, the reaction mixture was cooled, and water was added and extracted using ethyl acetate. To the organic layer, 10 M sodium hydroxide solution was added to remove any bisphenol residue present. The organic layer was dried over anhydrous sodium sulfate and evaporated under vacuum. The molecular structure of resultant products PYBP-dda, PYBP-oda, and PYBP-fa were analyzed using spectral studies.

The chemical structure of PYBP benzoxazine monomers (PYBP-dda, PYBP-oda, and PYBP-fa) was confirmed from the IR (Figure S4), NMR (Figure S5), and mass spectra (Figure S6).

FTIR spectra (Figure S4): 2915 and 2853 cm^{-1} [asymmetric and symmetric stretching vibrations of methylene group (–CH_2–) of oxazine ring as well as

long alkyl side chain of the dda and oda groups]. 916 cm^{-1} (benzoxazine ring).[49,50]

NMR spectra of PYBP-dda (Figure S5) ^{1}H-NMR δ ppm; 0.8–1.8 (multiplet, aliphatic protons), 2.4 (N-CO**$\underline{CH_3}$**), 2.7 (multiplet, *N*–CH_2– protons), δ 3.2, δ 3.7 and δ 5.4 (pyrazolidine ring protons), 3.8 and 4.0, 4.7 and 4.9 (two sets of singlets for benzoxazine ring): ^{13}C-NMR δ ppm: 20 (N-CO**$\underline{CH_3}$**), 59 and 83 (benzoxazine ring methylene carbons), 168 (N-**$\underline{CO}$**CH_3).

NMR spectra of PYBP-oda (Figure S5) ^{1}H-NMR δ ppm; 0.8–1.8 (multiplet, aliphatic protons), 2.4 (N-CO**$\underline{CH_3}$**), 2.7 (multiplet, *N*–CH_2– protons), δ 3.2, δ 3.7 and δ 5.4 (pyrazolidine ring protons), 3.8 and 4.0, 4.7 and 4.8 (two sets of singlets for benzoxazine ring): ^{13}C-NMR δ ppm: 20 (N-CO**$\underline{CH_3}$**), 59 and 83 (benzoxazine ring methylene carbons), 168 (N-**$\underline{CO}$**CH_3).

NMR spectra of PYBP-fa (Figure S5) ^{1}H-NMR δ ppm; 2.4 (N-CO**$\underline{CH_3}$**), δ 3.2, δ 3.7 and δ 5.4 (pyrazolidine ring protons), 4.5 and 4.6, 5.2 and 5.4 (two sets of singlets for benzoxazine ring) 6.6–7.8 (aromatic protons): ^{13}C-NMR δ ppm: 20 (N-CO**$\underline{CH_3}$**), 59 and 83 (benzoxazine ring methylene carbons), 156 and 159 (Ar-F attached quarternary carbons), 168 (N-**$\underline{CO}$**CH_3).

Synthesis of bisphenol-F-based benzoxazine monomer (BF-dda, BF-oda, BF-fa)

Bisphenol-F (10 g, 0.05 mol), respective amines [dodecylamine (dda)/octadecylamine (oda)/4-fluoroaniline (fa), 0.10 mol], and paraformaldehyde (6.6 g, 0.22 mol) were added separately to a round-bottom flask containing 1,4-dioxane (10 mL) and slightly warmed to 60°C to achieve homogeneity. Then the reaction temperature was raised to 110°C and stirred for 12 h. The progress of the reaction was monitored by TLC. After the formation of the product, the reaction mixture was cooled, and water was added and extracted using ethyl acetate. To the organic layer, 10 M sodium hydroxide solution was added to remove any residual bisphenol present. The organic layer was dried over anhydrous sodium sulfate and evaporated under vacuum (Scheme 2). The prepared benzoxazine monomers were labeled in accordance with IUPAC nomenclature as BF-dda, BF-oda, and BF-fa and were preserved for further studies.

The chemical structure of BPF benzoxazine monomers (BF-dda, BF-oda, and BF-fa) was confirmed from the IR (Figure S4), NMR (Figure S7), and mass spectra (Figure S8).

FTIR spectra (Figure S4): 2915 and 2853 cm^{-1} [asymmetric and symmetric stretching vibrations of methylene group (–CH_2–) of oxazine ring as well as long alkyl side chain of the dda and oda groups]. 916 cm^{-1} (benzoxazine ring).[49,50]

NMR spectra of BF-dda (Figure S7) ^{1}H-NMR δ ppm; 1.0–2.0 (multiplet, aliphatic protons), 2.7 (multiplet, *N*–CH_2– protons), 3.7 (CH_2 protons of BPF), 3.9 and 4.9 (two singlets, benzoxazine ring): ^{13}C-NMR δ ppm: 67 and 82 (benzoxazine ring methylene carbons), 60 (CH_2 carbon of BPF).

NMR spectra of BF-oda (Figure S7) ^{1}H-NMR δ ppm; 0.8–2.0 (multiplet, aliphatic protons), 2.6 (multiplet, *N*–CH_2– protons), 3.7 (CH_2 protons of BPF), 3.9 and 4.8 (two singlets, benzoxazine ring): ^{13}C-NMR δ ppm: 66 and 80 (benzoxazine ring methylene carbons), 60 (CH_2 carbon of BPF).

NMR spectra of BF-fa (Figure S7) ^{1}H-NMR δ ppm; 3.6 (CH_2 protons of BPF), 4.5 and 5.2 (two singlets, benzoxazine ring) 6.5–7.3 (aromatic protons): ^{13}C-NMR δ ppm: 60 (CH_2 carbon of BPF), 156 and 159 (Ar-F attached quarternary carbons).

Preparation of benzoxazine-coated mild steel

Electrochemical characterization was carried out using Biologic instrument, France. A three-electrode system was used consisting of mild steel specimens (2 cm × 1 cm) as the working electrode, stainless steel plate as the counter electrode, and Ag/AgCl (saturated KCl) as the reference electrode. Electrochemical corrosion studies were carried out using open-circuit potential, a potentiodynamic polarization method, and electrochemical impedance spectroscopy (EIS). All corrosion experiments were carried out in the corrosive medium containing 3.5% NaCl at room temperature. For polarization experiments, the scans were performed from − 250 mV below to + 250 mV above the open-circuit potential. The values of E_{corr} and I_{corr} were obtained directly from the Tafel plot using the EC-Lab software. Nyquist impedance analysis was carried out by applying a sinusoidal AC perturbation wave of 10 mV amplitude. The applied frequency ranged from 100 to 0.01 Hz. EIS analysis was done using EC-Lab software.

Preparation of the coatings

Uniform size mild steel plates having the size 2 cm × 1 cm were purchased from the local market. The mild steel plates were first thoroughly polished using emery papers and cleaned using acetone and dried. Exactly 1 g of the BF and PYBP monomers was weighed separately in a beaker, and 10 mL of THF was added and stirred for 10 min to completely dissolve the monomers. The mild steel was coated with the monomers by drop coating method and dried at room temperature for 5 h, and then it was cured in the air oven at 250°C for 5 h. The coating thickness was determined using SEM analysis and found to be about 20 μM (Figure S9).

Characterization

FTIR spectra measurements were carried out using an Agilent Cary 630 FTIR spectrometer. NMR spectra were recorded using a Bruker instrument (400 MHz) with deuterated chloroform ($CDCl_3$) and dimethylsulfoxide (DMSO-d_6) as a solvent and tetramethylsilane (TMS) as an internal standard. Mass spectra were recorded using an Agilent mass spectrometer. DSC measurements were recorded using NETZSCH STA 449F3 under N_2 purge (60 mL min^{-1}) at scanning rate of 10°C min^{-1}. Thermogravimetric analysis (TGA) was obtained using NETZSCH STA 449F3 using 5 mg of sample under N_2 flow (60 mL min^{-1}) at heating rate of 20°C min^{-1}. The morphology of the matrices and composites was analyzed from an FEI QUANTA 200F high-resolution scanning electron microscope (HRSEM). Contact angle measurements were carried out using a Kwoya goniometer with 5 μL of water as probe liquid.

Results and discussion

Toxicity studies

The toxicity studies of BPA, BPF, and the newly prepared pyrazolidine compound (PYBP) were carried out using Human Embryonic Kidney (HEK) cells by MTT [3-(4,5-dimethylthiazol-2-yl)-2,5-diphenyltetrazolium bromide] assay.[51] HEK cells were grown (1×10^4 cells/well) in a 96-well plate for 48 h into 75% confluence. The medium was replaced with fresh medium containing serially diluted synthesized compounds (10, 25, and 50 μg mL^{-1}), and the cells were further incubated for 48 h. The culture medium was removed, and 100 μL of the MTT [3-(4,5-dimethylthiozol-2-yl)-3,5-diphenyl tetrazolium bromide] (Hi-Media) solution was added to each well and incubated at 37°C for 4 h. After removal of the supernatant, 50 μL of dimethylsulfoxide was added to each of the wells and incubated for 10 min to solubilize the formazan crystals. The optical density (OD) was measured at 620 nm in an ELISA multiwell plate reader (Thermo Multiskan EX, USA). The OD value was used to calculate the percentage of viability using the following formula.

$$\% \text{ of viability} = \frac{\text{OD value of experimental sample}}{\text{OD value of experimental control}} \times 100 \quad (1)$$

As mentioned earlier, the toxicity of BPA restricts its application in various commercial products. There are few reports that state BPF also exhibits little toxicity.[38] In this regard, the newly prepared compound was analyzed for in vitro toxicity against HEK cells along with BPA and BPF. Figure S10 denotes the morphology of cell under control (without compound) condition and at different concentrations against BPA, BPF, and PYBP, respectively.

In all the controls, the cells are in normal structure. When the cells are treated with BPA, the morphology of the HEK cells is altered as observed in BPA (Figure S10). In the case of BPF, morphology of the HEK cells is also slightly altered, whereas the morphology of the HEK cells is not altered when they are treated with PYBP (Figure S10). The precise toxicity values in IC50 for the compounds BPA, BPF, and PYBP are presented in Table 1 and Figs. 1a–1c.

Table 1 presents the toxicity data of the compounds at 50% inhibition concentration or half maximal inhibitory concentration. Among the compounds, BPA shows IC_{50} = 15 μg mL^{-1} which is the same as the IC_{50} of Cisplatin, IC_{50} = 15 μg mL^{-1}. Next BPF also exhibits a moderate toxicity of IC_{50} = 37 μg mL^{-1}. Interestingly, the newly prepared compound PYBP does not exhibit any toxicity, IC_{50} > 100 μg mL^{-1}.

Curing behavior of benzoxazines

The ring opening polymerization of the prepared monomers is presented in Scheme 3. The lone pair on the nitrogen atom of the benzoxazine ring on heating drives the ring opening to create iminium nitrogen cation and a secondary carbanion. Further, the secondary carbanion on this unstable structure reacts with the iminium cation followed by keto-enol tautomerism that results in a polymer network. The thermograms of BPF and PYBP monomers obtained from DSC are presented in Figs. 2 and 3, respectively. The curing temperatures of the above monomers are presented in Table 2.

The curing onset of the BF-dda monomer starts at 183°C and ends at 273°C with the T_p at 249°C. However, the curing onset of the PYBP-dda monomer starts at 140°C and ends at 256°C with T_p at 198°C showing a decrease in the value of T_p of 50°C when compared to that of BF-dda. Similarly, the curing of BF-oda starts at 209°C and ends at 275°C with T_p of 239°C. The curing of PYBP-oda starts at 166°C and ends at 263°C with T_p of 209°C and again shows a decrease of 30°C in the value of T_p when compared to that of BF-oda. However, it was noticed that the

Table 1: Toxicity data (IC_{50}) of the compounds against human embryonic kidney cells

Compound	IC_{50} (μg mL^{-1})
BPA	15 ± 1.5
BPF	37 ± 1.0
PYBP	> 100
Cisplatin (standard)	15 ± 1.0

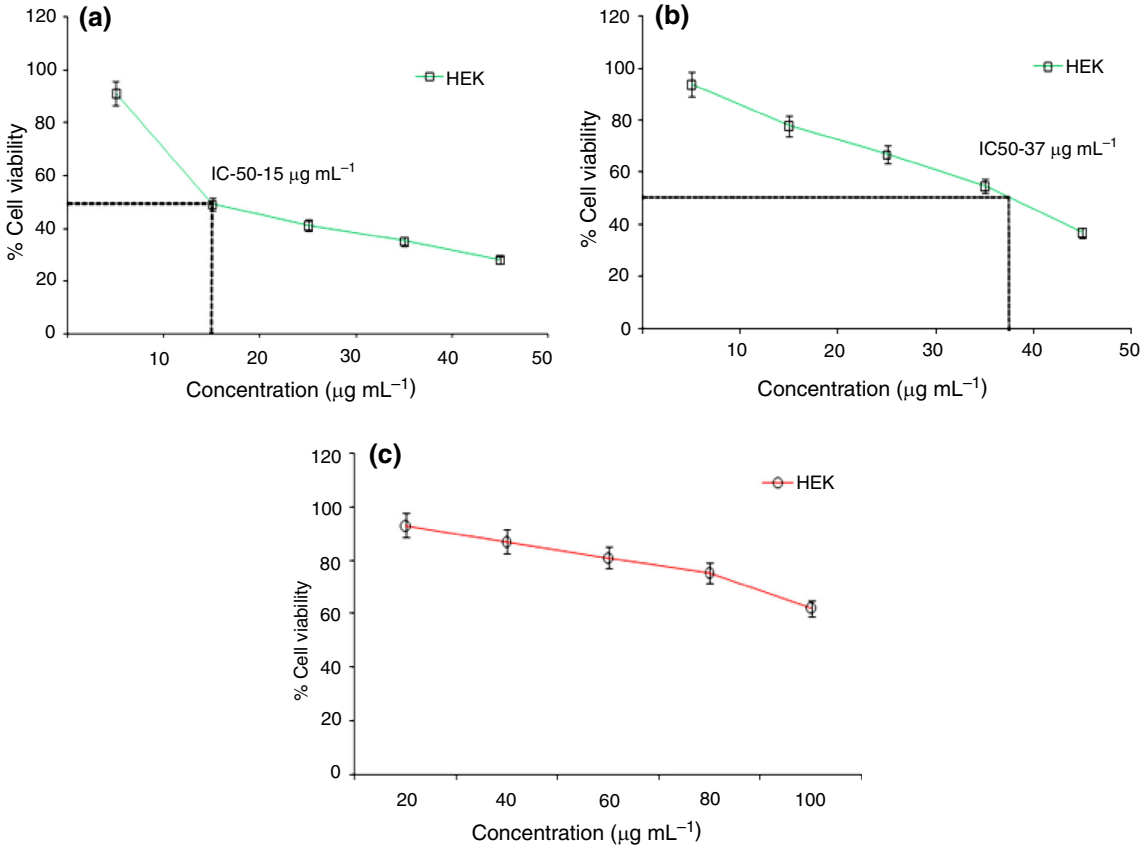

Fig. 1: Human embryonic kidney cell viability (IC_{50}) against compounds (a) BPA, (b) BPF, and (c) PYBP

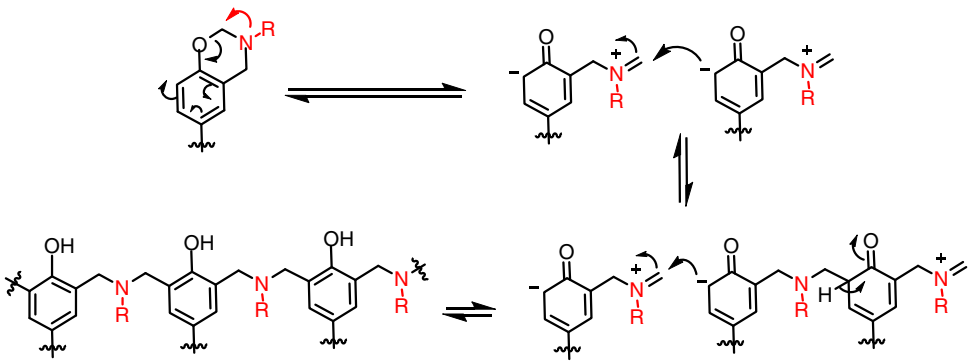

Scheme 3: General curing mechanism of benzoxazine monomer

fluoroaniline-based benzoxazines, BF-fa and PYBP, have a similar pattern of curing with T_p of 237 and 236°C, respectively. From the DSC analysis, it was observed that the curing temperatures of PYBP-based benzoxazines are comparatively lower than those of BPF-based benzoxazines. This might be due to the presence of amide bond of the *N*-acetyl group on the pyrazolidine ring which lowers the curing temperature.[52] In addition, the PYBP-based benzoxazine monomer liberates at a comparatively lower enthalpy than those of BF-based monomers.

In the FTIR spectra (Fig. 4), the disappearance of the peak at 916 cm^{-1} represents the occurrence of ring opening polymerization reaction. Further, the peak at 1463 cm^{-1} corresponds to the trisubstituted benzene ring of the polymer. The peaks observed at 2948 and

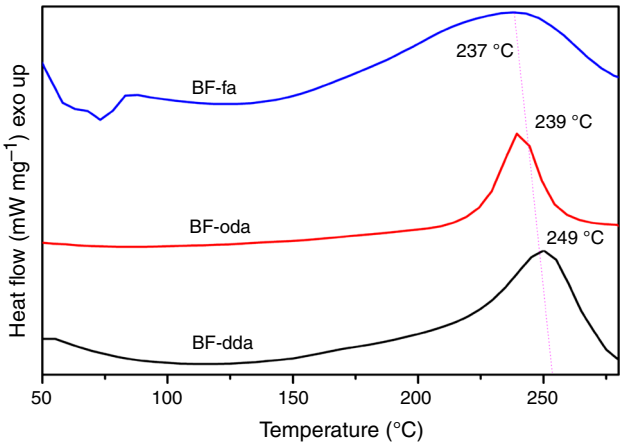

Fig. 2: DSC curing curve of BPF-based monomers

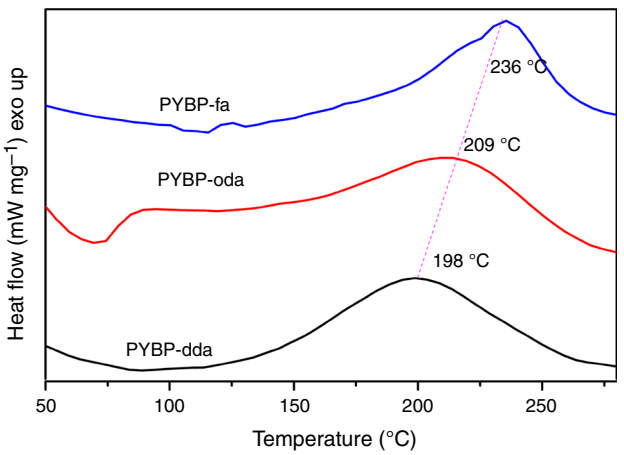

Fig. 3: DSC curing curve of PYBP-based monomers

Table 2: Curing behaviors of BPF and PYBP monomers

Monomers	T_i (°C)	T_p (°C)	T_{final} (°C)	ΔH (mJ mg^{-1})
BPF-dda	183	249	273	34
BPF-oda	209	239	275	35
BPF-fa	174	237	275	53
PYBP-dda	140	198	256	6
PYBP-oda	166	209	263	9
PYBP-fa	181	236	262	17

2893 cm^{-1} correspond to the asymmetric and symmetric stretching vibrations of methylene group (–CH_2–) of oxazine ring, respectively, as well as the long alkyl side chain of the dda and oda groups. The absence of peaks at 1242 and 1090 cm^{-1} for the C–O–C bond of the benzoxazine monomer and the absence of peak at 1152 cm^{-1} for the asymmetric stretching of C–N–C of benzoxazine monomer clearly infer the occurrence of curing reactions.

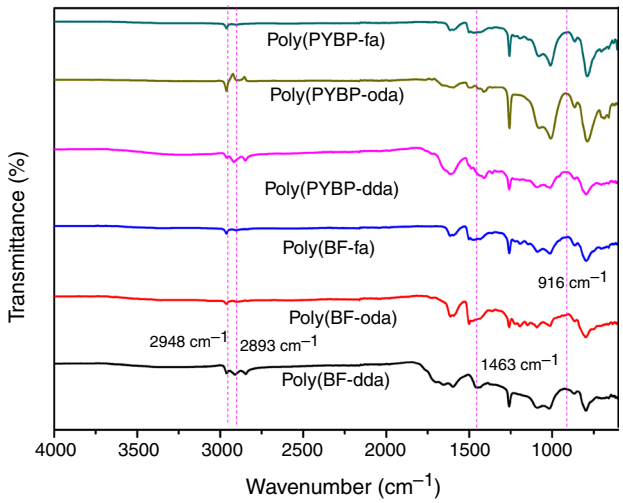

Fig. 4: FTIR spectra of BPF and PYBP-based polybenzoxazines

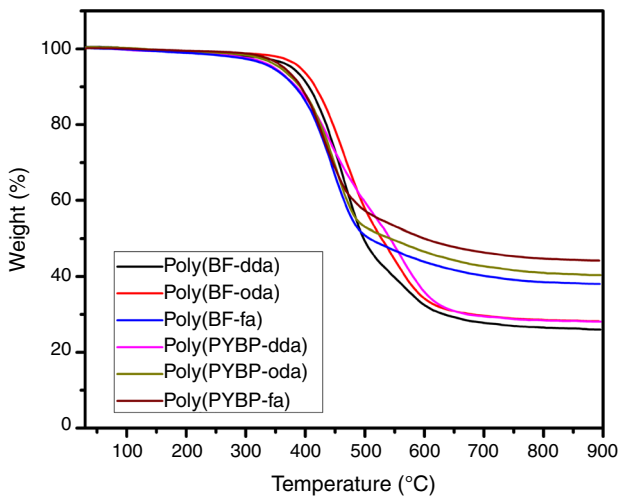

Fig. 5: TGA of BPF and PYBP-based polybenzoxazines

Thermal behavior

The thermal stability of polymeric materials enhances their industrial utility mainly for high temperature and flame retardant applications. Hence, it is highly desirable to assess the thermal behavior of benzoxazines prepared in the present work. The thermal stability was studied using TGA and the data obtained are presented in Fig. 5 and Table 3.

The thermal degradation temperatures corresponding to 5% and 10% weight loss are presented in Table 3 along with the char yield obtained at 900°C. The poly(BF-dda), poly(BF-oda), and poly(BF-fa) showed 5% weight loss at 378, 391, and 396°C, respectively, and the poly(PYBP-dda), poly(PYBP-oda), and poly(PYBP-fa) showed 5% weight loss at 340, 362, and 365°C, respectively. The results were in a similar pattern for 10% weight loss. However, the maximum degradation temperatures for poly(BF-dda),

Table 3: Thermal behaviors of benzoxazines

Sample	Degradation temperature (°C)			Char yield % at 900°C	LOI
	$T_{-5\%}$	$T_{-10\%}$	T_{max}		
Poly(BF-dda)	378	406	449	26	27.9
Poly(BF-oda)	391	414	461	29	29.1
Poly(BF-fa)	396	415	471	38	32.7
Poly(PYBP-dda)	340	373	422	28	28.7
Poly(PYBP-oda)	362	391	471	40	33.5
Poly(PYBP-fa)	365	395	510	44	35.1

poly(BF-oda), and poly(BF-fa) were 449, 461, and 471°C which were quite similar to that of poly(PYBP-dda), poly(PYBP-oda), and poly(PYBP-fa) having maximum degradation temperatures of 422, 471, and 510°C, respectively. Even though the 5% and 10% weight loss temperatures for BPF-based benzoxazine matrices were higher when compared to that of PYBP-based benzoxazine matrices, the T_{max} temperatures of both the benoxazines were quite similar and higher than 400°C. On the other hand, the char yields of poly(BF-dda), poly(BF-oda), and poly(BF-fa) at 900°C were 26%, 29%, and 38%, respectively, whereas the char yields of poly(PYBP-dda), poly(PYBP-oda), and poly(PYBP-fa) were 28%, 40%, and 44%, respectively. It is significant to mention that the char yields of the PYBP-based benzoxazines were higher than that of the BPF-based benzoxazines, and this value directly influences and contributes to enhanced values of LOI. The LOI values were calculated using the Van Krevelen and Hoftyzer relation between the char yield and LOI, which is given in equation (2).[53]

$$\mathrm{LOI} = 17.5 + 0.4(\mathrm{CR}) \quad (2)$$

Here, CR is the percentage char yield of the sample remaining at 850°C. It is experimentally proven that the materials having higher LOI values are flame retardant in nature. The LOI of poly(BF-dda), poly(BF-oda), and poly(BF-fa) were 27.9, 29.1, and 32.7, respectively, whereas the LOI of poly(PYBP-dda), poly(PYBP-oda), and poly(PYBP-fa) were 28.7, 33.5, and 35.1, respectively. In the case of the pyrazolidine-based benzoxazines, the poly(PYBP-oda) and poly(PYBP-fa) possessed the highest char yield and LOI values, which might be due to the presence of thermally stable pyrazolidine heterocyclic core and fluorine atom of the aromatic side chain.

Morphological properties of polybenzoxazines

In order to ascertain the microstructure of both BPF and PYBP-based benzoxazines, the scanning electron microscopic (SEM) images were taken and are presented in Fig. 6. Interestingly, poly(BF-dda) and poly(BF-oda) as well as poly(PYBP-dda) and poly(PYBP-oda) showed roughness on their surfaces when compared to those of poly(BF-fa) and poly(PYBP-fa). In particular, the poly(BF-oda) and poly(PYBP-oda) showed wrinkled ripples morphology. The long-chain octadecylamine present in both cases showed jagged protrusion (Figs. 6b and 6e). These rough surfaces can thus repel the water causing hydrophobicity. In the case of 4-fluoroaniline monomers, poly(BF-fa) and poly(PYBP-fa) showed only smooth surfaces as attributed from Figs. 6c and 6f, respectively.

The water contact angle (WCA) values of the polymer-coated MS specimens obtained are presented in Fig. 7. The WCA of uncoated MS was 58.6°. The WCA of the MS coated with poly(BPF-dda), poly(BPF-oda), and poly(BPF-fa) were 92.4°, 100.3°, and 77.6°, respectively. The octadecyl long-chain-based poly(BPF-oda) showed higher WCA, due to the hydrophobic nature of the alkyl chain. Whereas, in the case of poly(PYBP)-based benoxazines, the WCA of the MS-coated with poly(PYBP-dda), poly(PYBP-oda), and poly(PYBP-fa) were 99.8°, 111.2°, and 85.8°, respectively. Here also the octadecyl alkyl chain influenced the WCA to 111.2° which was the highest value observed among the different benzoxazines prepared in the present work. The poly(PYBP-oda) prepared in the present work can be used as a better coating material on the surface of MS to create hydrophobicity.

Morphological properties of polybenzoxazine-coated mild steel

After being coated with mild steel, the SEM images of the plates were taken and are shown in Figs. 8a–8e. From these figures, it is clear that the plates coated show roughness, particularly in the cases of poly(BF-oda) and poly(PYBP-oda) holding a hydrophobic long-chain octadecyl group. The existence of the roughness on the surfaces of the MS coated with poly(BF-oda) and poly(PYBP-oda) is the possible reason for having higher hydrophobicity and in turn, a higher WCA value.

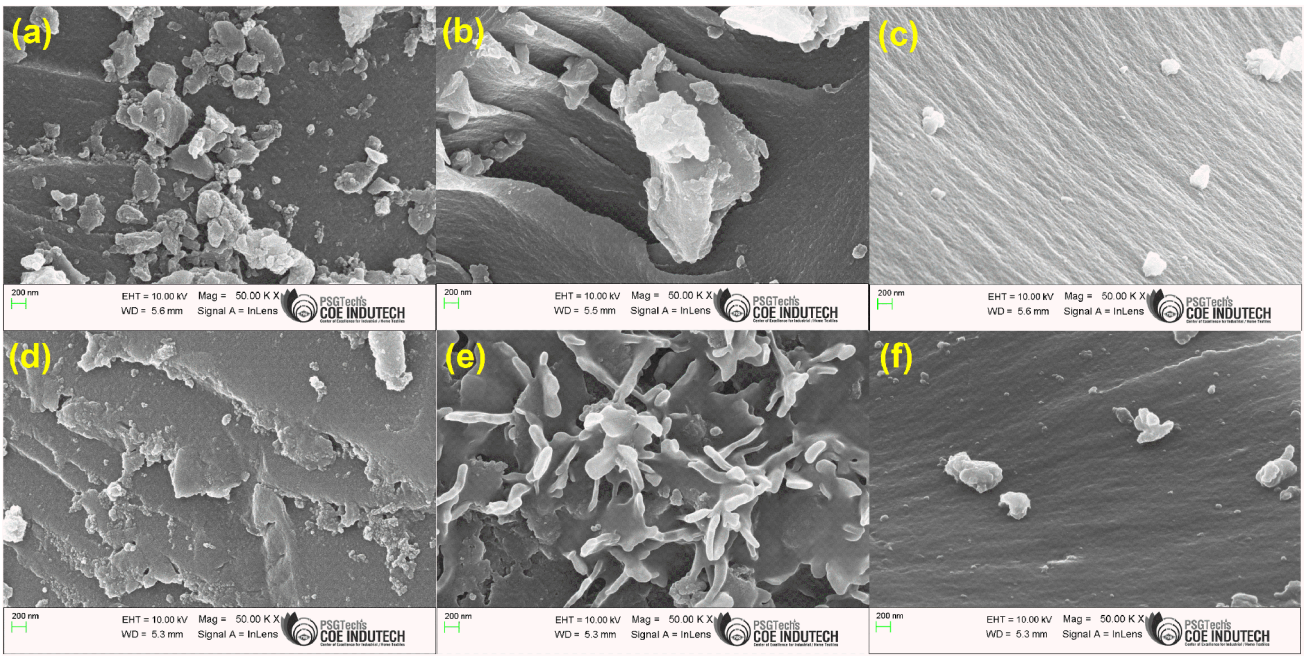

Fig. 6: SEM images of (a) poly(BF-dda), (b) poly(BF-oda), (c) poly(BF-fa), (d) poly(PYBP-dda), (e) poly(PYBP-oda), (f) poly(PYBP-fa)

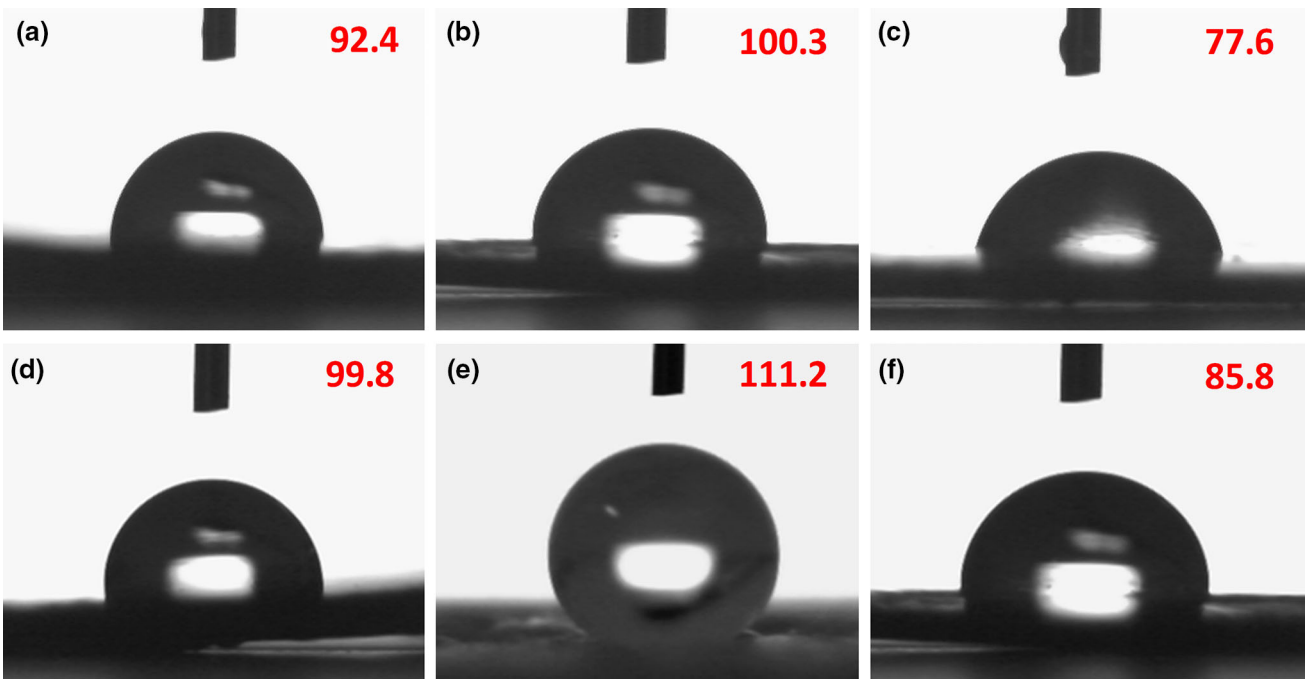

Fig. 7: Water contact angle images of (a) poly(BF-dda), (b) poly(BF-oda), (c) poly(BF-fa), (d) poly(PYBP-dda), (e) poly(PYBP-oda), (f) poly(PYBP-fa)

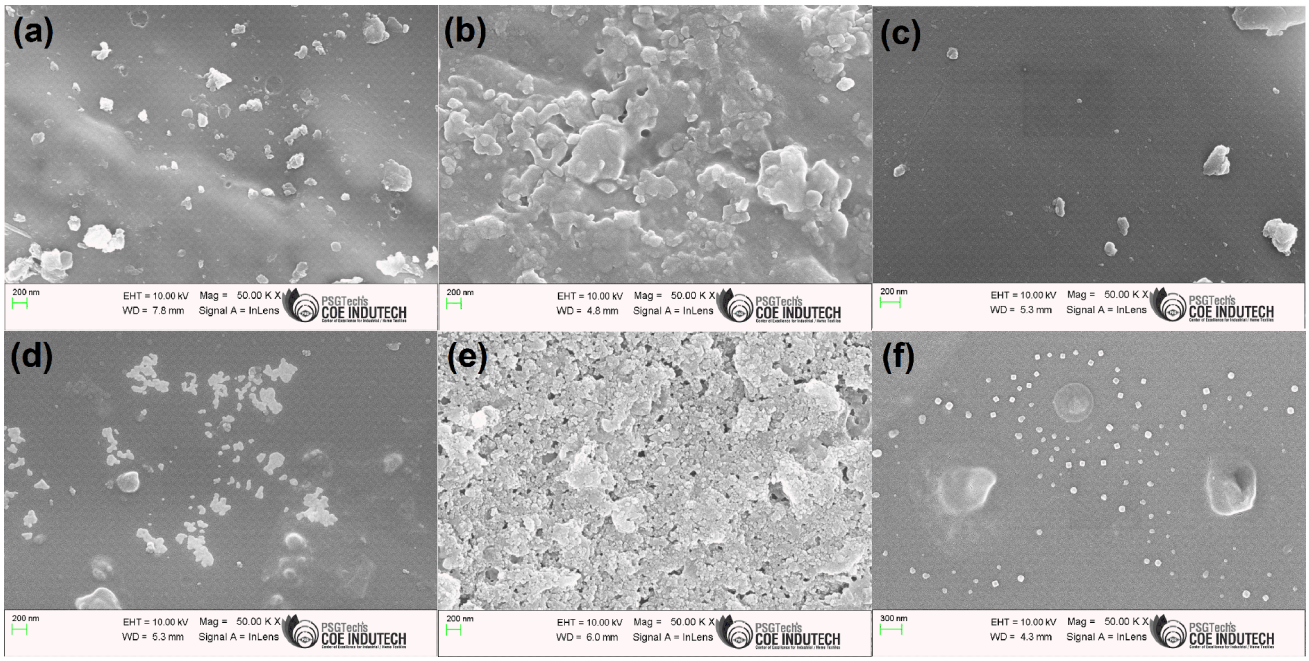

Fig. 8: SEM images of mild steel coated with (a) poly(BF-dda), (b) poly(BF-oda), (c) poly(BF-fa), (d) poly(PYBP-dda), (e) poly(PYBP-oda), (f) poly(PYBP-fa)

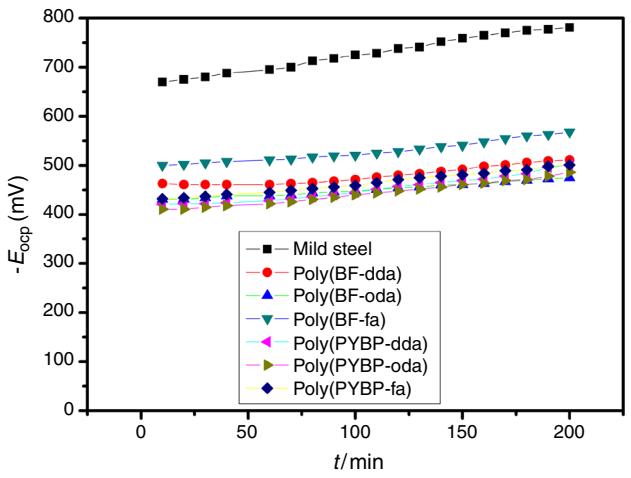

Fig. 9: Plot of E_{ocp} vs time in 3.5% of NaCl solution for different mild steel specimens

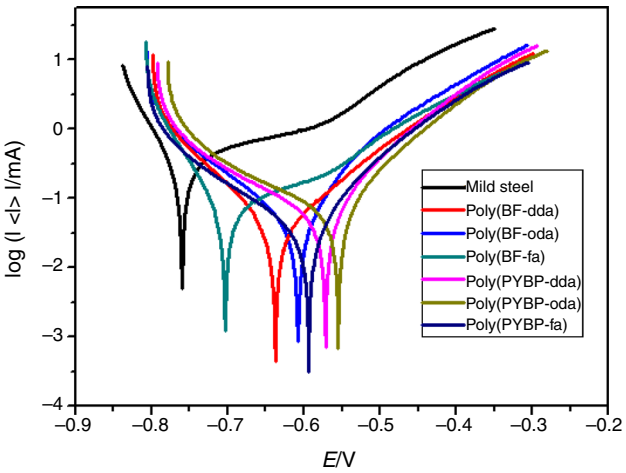

Fig. 10: Linear polarization curves for bare mild steel plates and polybenzoxazine-coated plates in 3.5% NaCl solution

Electrochemical studies of the coated and uncoated mild steel specimens: open-circuit potential (E_{ocp}) analysis

The effectiveness of the coating was assessed with the help of open-circuit potential (E_{ocp}) measured for the mild steel immersed in 3.5% NaCl medium. The plot of E_{ocp} vs time is shown in Fig. 9. The E_{ocp} is one of the key parameters to obtain an idea about the nature of the film formed on the steel plates.[54] E_{ocp} for the uncoated mild steel specimen was around − 670 mV. The E_{ocp} values of the coated specimens shifted toward the anodic region by nearly 200 mV. The tendency of the E_{ocp} to shift toward the anodic direction is the indication of high corrosion resistance offered by coatings formed on the electrode surface which prevents the diffusion of the corrosive species in the film. A greater shift was noticed in the case of poly(PYBP-oda)-coated specimen, which possessed more corrosion

resistance behavior when compared to that of other coated specimens and bare mild steel specimen.

Polarization and electrochemical impedance studies of coated and uncoated mild steel specimens

The kinetics of the anodic and cathodic corrosion reactions have been studied using the potentiodynamic polarization method. Tafel plots of the coated and uncoated mild steel specimens are shown after 48 h of immersion time in 3.5% NaCl solution (Fig. 10).

The corrosion parameters such as corrosion potential E_{corr}, corrosion current i_{corr}, and cathodic and anodic Tafel slopes have been obtained by the extrapolation of Tafel curves.[54] The obtained parameters are presented in Table 4. Tafel extrapolations indicate that the polymer-coated specimens show a positive shift of around 200 mV in the corrosion potential when compared to that of bare mild steel specimen. As corrosion potential E_{corr} shifts toward the anodic region (noble region), the corrosion resistance also increased.[55–59] From the Tafel plot, it can be noted that the surface of the mild steel specimen has more corrosion resistance behavior after coating. In addition, the corrosion current for the coated specimens decreased significantly when compared to that of bare mild steel specimen. The lower polarization current supports the better corrosion resistance of the coatings.[60] All these polymers possess an effective corrosion-resistant behavior and prevent corrosion on the surface of the mild steel. From the Tafel plot, it can also be seen that poly(BF-oda)-coated MS shows better corrosion resistance when compared to that of the other two poly(BF-dda) and poly(BF-fa)-coated specimens. This may be due to the presence of the hydrophobic long alkyl chain. Similarly, in the case of poly(PYBP) series, poly(PYBP-oda) exhibited more positive E_{corr} value and less corrosion current which corroborates the observation made in the OCP curves. This is due to the presence of pyrazoline ring with enriched nitrogen and *N*-acetyl group which increases the interactive forces of the polymer with the mild steel specimen, thus leading to the formation of adherent coating which prevents the intrusion of the corrosive medium into the coating metal interface. The efficiency (η) of the corrosion coating is calculated using the following equation (3),

$$\eta = \frac{i_{corr}(\text{blank}) - i_{corr}(\text{coated})}{i_{corr}(\text{blank})} \times 100 \quad (3)$$

where i_{corr} (blank) and i_{corr} (coated) are the corrosion current density of bare MS specimen and that of specimens coated with benzoxazines, respectively.[61] Normally, corrosion will take place when there is a diffusion of the corrosive medium into the coating metal interface due to the presence of small pores in the coating or delamination of the coating due to instability of the film in the corrosive medium. This induces the oxidation and reduction reactions to occur at the metal–coating interface, which causes the corrosion phenomenon to take place on metal substrate.

At the anode, oxidation of the metal takes place

$$Fe \rightarrow Fe^{2+} + 2e^{-} \quad (4)$$

At the cathode, reduction reaction takes place

$$O_2 + 2H_2O + 4e^{-} \rightarrow 4OH^{-} \quad (5)$$

The product of the overall reaction of the anode and the cathode presented in equations (4) and (5) is $Fe(OH)_2$. The adherent coating offered by the prepared polybenzoxazines will thus prevent the contact of oxygen/electrolyte to the metallic surface. Hence the occurrence of the above reaction is inhibited. The efficiency of poly(BF-dda), poly(BF-oda), and poly(BF-fa) calculated from equation (3) were 83.44%, 85.52%, and 82.06%, respectively. Similarly, the efficiency of poly(PYBP-dda), poly(PYBP-oda), and poly(PYBP-fa) were 87.60%, 90.00%, and 84.13%, respectively. In both the series, the PBz holding hydrophobic octadecyl chain displayed higher efficiency values for corrosion resistance coating than that of other dodecyl chain or 4-fluoroaryl chain-based benzoxazine samples.

Electrochemical impedance spectroscopy (EIS) is an important tool to investigate the coatings. Nyquist plots derived from the EIS measurements for the

Table 4: Potentiodynamic polarization studies of the coated and uncoated mild steel specimens in 3.5% NaCl solution

Specimens	E_{corr} (mV)	I_{corr} (μA)	β_a (mV)	β_c (mV)	Efficiency η (%)
Bare MS	− 763	145	170	83	–
Poly(BF-dda)	− 642	24	109	77	83.44
Poly(BF-oda)	− 610	21	79	63	85.52
Poly(BF-fa)	− 704	26	78	78	82.06
Poly(PYBP-dda)	− 582	18	74	110	87.60
Poly(PYBP-oda)	− 557	15	72	106	90.00
Poly(PYBP-fa)	− 593	23	85	122	84.13

coated and uncoated mild steel specimens in 3.5% NaCl solution are shown in Fig. 11. The corrosion-resistant behaviors of all samples were discussed in terms of coating resistance (R_c), solution resistance (R_s), coating capacitance (C_c), charge transfer resistance (R_{ct}), double-layer capacitance (C_{dl}), and constant phase element representing double-layer capacitance (Q_{dl}).[62,63] Hence, fitting of all EIS data is done using the equivalent circuit model represented in Figs. 12a and 12b.

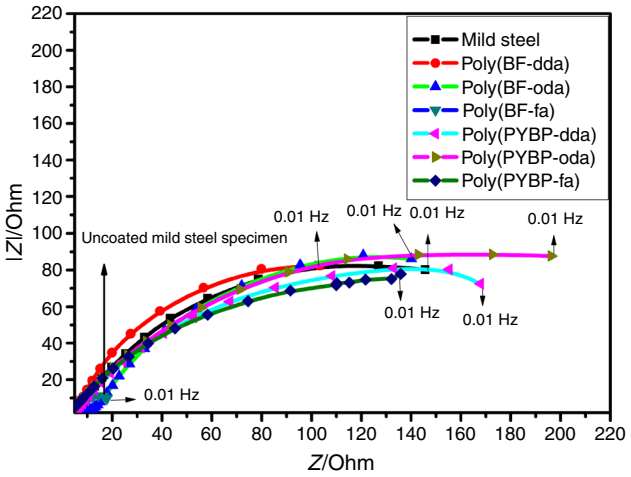

Fig. 11: Nyquist plot of coated and uncoated mild steel specimens in 3.5% NaCl solution

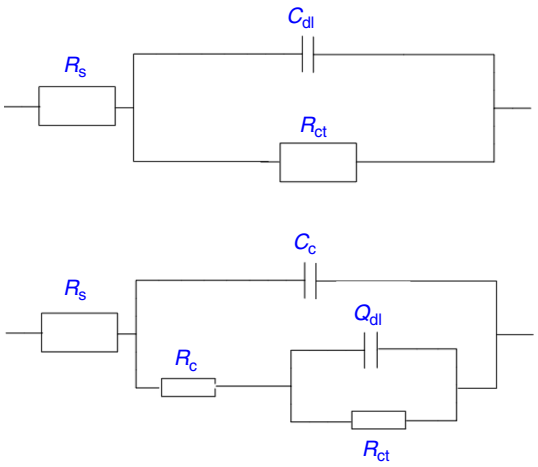

Fig. 12: Equivalent electrical circuit used to fit the electrochemical impedance spectroscopy

In fact, when an electrode is in contact with the electrolyte solution, a double layer forms. The formation of the double layer can be analyzed with the help of EIS data in terms of semicircles. The double layer is considered to be the capacitor in the equivalent circuit. In the real capacitor, electrons are responsible for charge accumulation which gives a perfect semicircle. In double-layer capacitors, electrons from the metal side and ions from the solution side are responsible for double layer formation. Actually, several factors affect the formation of a perfect semicircle such as greater volume of the ions than the electrons, roughness of the electrode, surface and mass transfer resistance in the system.[58] Hence, a deformed Nyquist curve (incomplete semicircle) is obtained.[55,64,65] As expected in the EIS theory, all the coated and uncoated MS specimens give an incomplete semicircle. The impedance parameters are obtained by fitting using EC-Lab software. The data obtained are presented in Table 5. The R_c and R_{ct} values of all the coated specimens increase when compared to that of uncoated specimen. Among the polymer-coated mild steel specimens, the dodecyl chain moieties, namely poly(BF-oda) and poly(PYBP-oda), have a capacitive loop with greater diameter and obviously they have maximum R_c and R_{ct} values. In particular, the poly(PYBP-oda) showed greater R_c and R_{ct} values of 220 and 381 kΩ cm^{-2}, respectively. This film offers a high compact coating when compared to that of the rest of the samples. For bare MS (uncoated specimen), a very small capacitive loop was obtained which has a lower R_{ct} value of 11 kΩ cm^{-2}. The results obtained in EIS are in good agreement with Tafel and OCP results. Further, the results obtained were also comparable with the results from the earlier literature.[29,54] The promising results of the poly(PYBP-oda) indicate that the newly developed polybenzoxazine discussed in the present study can be used as an effective corrosion-resistant material for mild steel under

Table 5: Parameters of corrosion and impedance kinetics

Samples	R_s (Ω cm^2)	CPE_c		R_c (kΩ cm^2)	CPE_{dl}		R_{ct} (kΩ cm^2)
		($F\ s^{n-1}$)	n		($F\ s^{n-1}$)	n	
Bare MS	6.34	05.75 × e^{-2}	0.878	1.3	11.64 × e^{-3}	0.737	11
Poly(BF-dda)	08.94	01.30 × e^{-2}	0.803	25	02.26 × e^{-3}	0.897	210
Poly(BF-oda)	09.83	08.03 × e^{-3}	0.773	51	01.03 × e^{-2}	0.781	278
Poly(BF-fa)	03.78	16.07 × e^{-3}	0.904	15	08.03 × e^{-3}	0.560	146
Poly(PYBP-dda)	09.23	24.04 × e^{-3}	0.649	75	07.90 × e^{-4}	0.993	287
Poly(PYBP-oda)	09.21	02.24 × e^{-4}	0.540	220	02.70 × e^{-4}	0.725	381
Poly(PYBP-fa)	08.25	10.13 × e^{-3}	0.661	58	02.58 × e^{-3}	0.872	227

different conditions. The nontoxic nature of the poly(PYBP-oda) could also extend its application to the marine environment.

Conclusion

The replacement of toxic bisphenol-A-based benzoxazine with nontoxic pyrazolidine-based benzoxazine (PYBP) or less toxic bisphenol-F (BPF) and their application toward corrosion resistance on mild steel was achieved. The new PYBP series displayed a low curing temperature of about 30–50°C when compared to those of BPF-based benzoxazines. The thermal properties of poly(PYBP-oda) (char yield = 40%, LOI = 33.5) and poly(PYBP-fa) (char yield = 44%, LOI = 35.1) were also higher when compared to those of poly(BPF-oda) (char yield = 29%, LOI = 32.2) and poly(BPF-fa) (char yield = 38%, LOI = 32.2). Further, the prepared PBzs were coated on mild steel to investigate their efficiency toward corrosion resistance in 3.5% NaCl solution. The corrosion protection behavior of the coated specimens were carried out using open-circuit potential (OCP), electrochemical impedance spectroscopy (EIS), and potentiodynamic polarization. The results obtained from Tafel and Nyquist plots indicated that the polybenzoxazine-coated mild steel possessed an excellent corrosion resistance behavior when compared to that of uncoated mild steel. Among the coated mild steel specimens studied, the poly(PYBP-oda)-coated specimen offered better corrosion protection behavior and possessed an efficiency of 90% and higher charge transfer resistance (R_{ct}) of 381 kΩ cm^2. The promising results of the poly(PYBP-oda) indicate that the newly developed polybenzoxazine discussed in the present study can be used as an effective corrosion-resistant material for mild steel under different conditions including marine environment.

Acknowledgments The authors thank the PSG Management, Coimbatore, India for their moral and financial support.

Conflict of interest The authors have no conflict of interest.

References

1. Döner, A, Solmaz, R, Özcan, M, Kardaş, G, ''Experimental and Theoretical Studies of Thiazoles as Corrosion Inhibitors for Mild Steel in Sulphuric Acid Solution.'' *Corros. Sci.*, **53** (9) 2902–2913 (2011)
2. Baddoo, NR, ''Stainless Steel in Construction: A Review of Research, Applications, Challenges and Opportunities.'' *J. Constr. Steel Res.*, **64** (11) 1199–1206 (2008)
3. Wang, Y, Wang, W, Liu, Y, Zhong, L, Wang, J, ''Study of Localized Corrosion of 304 Stainless Steel Under Chloride Solution Droplets Using the Wire Beam Electrode.'' *Corros. Sci.*, **53** (9) 2963–2968 (2011)
4. Prasai, D, Tuberquia, JC, Harl, RR, Jennings, GK, Bolotin, KI, ''Graphene: Corrosion-Inhibiting Coating.'' *ACS Nano*, **6** (2) 1102–1108 (2012)
5. Liu, M, Mao, X, Zhu, H, Lin, A, Wang, D, ''Water and Corrosion Resistance of Epoxy-Acrylic-Amine Waterborne Coatings: Effects of Resin Molecular Weight, Polar Group and Hydrophobic Segment.'' *Corros. Sci.*, **75** 106–113 (2013)
6. Rahman, OU, Ahmad, S, ''Physico-Mechanical and Electrochemical Corrosion Behavior of Soy Alkyd/Fe_3O_4 Nanocomposite Coatings.'' *RSC Adv.*, **4** (29) 14936–14947 (2014)
7. Sun, W, Wang, L, Wu, T, et al., ''Inhibiting the Corrosion-Promotion Activity of Graphene.'' *Chem. Mater.*, **27** (7) 2367–2373 (2015)
8. Sharmin, E, Zafar, F, Akram, D, Alam, M, Ahmad, S, ''Recent Advances in Vegetable Oils Based Environment Friendly Coatings: A Review.'' *Ind. Crops Prod.*, **76** 215–229 (2015)
9. Gnedenkov, SV, Sinebryukhov, SL, Mashtalyar, DV, Egorkin, VS, Sidorova, MV, Gnedenkov, AS, ''Composite Polymer-Containing Protective Coatings on Magnesium Alloy MA8.'' *Corros. Sci.*, **85** 52–59 (2014)
10. Qi, K, Sun, Y, Duan, H, Guo, X, ''A Corrosion-Protective Coating Based on a Solution-Processable Polymer-Grafted Graphene Oxide Nanocomposite.'' *Corros. Sci.*, **98** 500–506 (2015)
11. Deshpande, PP, Jadhav, NG, Gelling, VJ, Sazou, D, ''Conducting Polymers for Corrosion Protection: A Review.'' *J. Coat. Technol. Res.*, **11** (4) 473–494 (2014)
12. Krishnadevi, K, Selvaraj, V, ''Cyclotriphosphazene and TiO_2 Reinforced Nanocomposite Coated on Mild Steel Plates for Antibacterial and Corrosion Resistance Applications.'' *Appl. Surf. Sci.*, **366** 148–157 (2016)
13. Riaz, U, Nwaoha, C, Ashraf, SM, ''Recent Advances in Corrosion Protective Composite Coatings Based on Conducting Polymers and Natural Resource Derived Polymers.'' *Prog. Org. Coat.*, **77** (4) 743–756 (2014)
14. Lu, X, Liu, Y, Zhou, C, Zhang, W, Xin, Z, ''Corrosion Protection of Hydrophobic Bisphenol A-Based Polybenzoxazine Coatings on Mild Steel.'' *RSC Adv.*, **6** (7) 5805–5811 (2016)
15. Zhou, C, Lu, X, Xin, Z, Liu, J, Zhang, Y, ''Hydrophobic Benzoxazine-Cured Epoxy Coatings for Corrosion Protection.'' *Prog. Org. Coat.*, **76** (9) 1178–1183 (2013)
16. Hosseini, M, Mertens, SFL, Ghorbani, M, Arshadi, MR, ''Asymmetrical Schiff Bases as Inhibitors of Mild Steel Corrosion in Sulphuric Acid Media.'' *Mater. Chem. Phys.*, **78** (3) 800–808 (2003)
17. Subramanyam, NC, Sheshadri, BS, Mayanna, SM, ''Thiourea and Substituted Thioureas as Corrosion Inhibitors for Aluminium in Sodium Nitrite Solution.'' *Corros. Sci.*, **34** (4) 563–571 (1993)
18. Shi, X, Nguyen, TA, Suo, Z, Liu, Y, Avci, R, ''Effect of Nanoparticles on the Anticorrosion and Mechanical Properties of Epoxy Coating.'' *Surf. Coat. Technol.*, **204** (3) 237–245 (2009)
19. Zaferani, SH, Zaarei, D, Danaee, I, Mehrabian, N, ''The Effect of Organosilane on Corrosion Resistance of Epoxy Coating Containing Cerium Nitrate.'' *J. Adhes. Sci. Technol.*, **28** (2) 151–160 (2014)
20. Ganjaee Sari, M, Ramezanzadeh, B, Shahbazi, M, Pakdel, AS, ''Influence of Nanoclay Particles Modification by Polyester-Amide Hyperbranched Polymer on the Corrosion

Protective Performance of the Epoxy Nanocomposite.'' *Corros. Sci.*, **92** 162–172 (2015)
21. Ghosh, NN, Kiskan, B, Yagci, Y, ''Polybenzoxazines—New High Performance Thermosetting Resins: Synthesis and Properties.'' *Prog. Polym. Sci.*, **32** (11) 1344–1391 (2007)
22. Vengatesan, MR, Devaraju, S, Dinakaran, K, Alagar, M, ''SBA-15 Filled Polybenzoxazine Nanocomposites for Low-*k* Dielectric Applications.'' *J. Mater. Chem.*, **22** (15) 7559–7566 (2012)
23. Ishida, H, Low, HY, ''A Study on the Volumetric Expansion of Benzoxazine-Based Phenolic Resin.'' *Macromolecules*, **30** (4) 1099–1106 (1997)
24. Dumas, L, Bonnaud, L, Olivier, M, Poorteman, M, Dubois, P, ''High Performance Benzoxazine/CNT Nanohybrid Network—An Easy and Scalable Way to Combine Attractive Properties.'' *Eur. Polym. J.*, **58** 218–225 (2014)
25. Arslan, M, Kiskan, B, Yagci, Y, ''Benzoxazine-Based Thermosets with Autonomous Self-Healing Ability.'' *Macromolecules*, **48** (5) 1329–1334 (2015)
26. Zhou, C, Lin, J, Lu, X, Xin, Z, ''Enhanced Corrosion Resistance of Polybenzoxazine Coatings by Epoxy Incorporation.'' *RSC Adv.*, **6** (34) 28428–28434 (2016)
27. Kiskan, B, Ghosh, NN, Yagci, Y, ''Polybenzoxazine-Based Composites as High-Performance Materials.'' *Polym. Int.*, **60** (2) 167–177 (2011)
28. Ishida, H, Agag, T, *Handbook of Benzoxazine Resins*. Elsevier, Boca Raton (2011)
29. Zhou, C, Lu, X, Xin, Z, Liu, J, Zhang, Y, ''Polybenzoxazine/SiO_2 Nanocomposite Coatings for Corrosion Protection of Mild Steel.'' *Corros. Sci.*, **80** 269–275 (2014)
30. Lin, SC, Wu, CS, Yeh, JM, Liu, YL, ''Reaction Mechanism and Synergistic Anticorrosion Property of Reactive Blends of Maleimide-Containing Benzoxazine and Amine-Capped Aniline Trimer.'' *Polym. Chem.*, **5** (14) 4235–4244 (2014)
31. Okada, H, Tokunaga, T, Liu, X, Takayanagi, S, Matsushima, A, Shimohigashi, Y, ''Direct Evidence Revealing Structural Elements Essential for the High Binding Ability of Bisphenol A to Human Estrogen-Related Receptor-γ.'' *Environ. Health Perspect.*, **116** (1) 32–38 (2008)
32. Lehmler, HJ, Liu, B, Gadogbe, M, Bao, W, ''Exposure to Bisphenol A, Bisphenol F, and Bisphenol S in U.S. Adults and Children: The National Health and Nutrition Examination Survey 2013–2014.'' *ACS Omega.*, **3** (6) 6523–6532 (2018)
33. Vermeirssen, ELM, Dietschweiler, C, Werner, I, Burkhardt, M, ''Corrosion Protection Products as a Source of Bisphenol A and Toxicity to the Aquatic Environment.'' *Water Res.*, **123** 586–593 (2017)
34. Tišler, T, Erjavec, B, Kaplan, R, Şenilă, M, Pintar, A, ''Unexpected Toxicity to Aquatic Organisms of Some Aqueous Bisphenol A Samples Treated by Advanced Oxidation Processes.'' *Water Sci. Technol.*, **72** (1) 29–37 (2015)
35. U.S. Food and Drug Administration; Food additives and Petitions; Bisphenol A, content current as of 06/27/2018. https://www.fda.gov/food/food-additives-petitions/bisphenol-bpa.
36. The Express Wire press release ''Bisphenol F Epoxy Resins Market 2019 Supply-Demand, Absolute Reports and End UserAnalysis to 2024''. https://www.theexpresswire.com/pressrelease/Bisphenol-F-Epoxy-Resins-Market-2019-Supply-Demand-Absolute-Reports-and-End-User-Analysis-to-2024_10222604 (posted on march 27, 2019)
37. Liu, J, Ishida, H, ''Anomalous Isomeric Effect on the Properties of Bisphenol F-Based Benzoxazines: Toward the Molecular Design for Higher Performance.'' *Macromolecules*, **47** (16) 5682–5690 (2014)
38. Rochester, JR, Bolden, AL, ''Bisphenol S and F: A Systematic Review and Comparison of the Hormonal Activity of Bisphenol A Substitutes.'' *Environ. Health Perspect.*, **123** (7) 643–650 (2015)
39. Salum, ML, Iguchi, D, Arza, CR, Han, L, Ishida, H, Froimowicz, P, ''Making Benzoxazines Greener: Design, Synthesis, and Polymerization of a Biobased Benzoxazine Fulfilling Two Principles of Green Chemistry.'' *ACS Sustain. Chem. Eng.*, **6** (10) 13096–13106 (2018)
40. Ergin, M, Kiskan, B, Gacal, B, Yagci, Y, ''Thermally Curable Polystyrene via Click Chemistry.'' *Macromolecules*, **40** (13) 4724–4727 (2007)
41. Kukut, M, Kiskan, B, Yagci, Y, ''Self-Curable Benzoxazine Functional Polybutadienes Synthesized by Click Chemistry.'' *Des. Monomers Polym.*, **12** (2) 167–176 (2009)
42. Nagai, A, Kamei, Y, Wang, XS, et al., ''Synthesis and Crosslinking Behavior of a Novel Linear Polymer Bearing 1,2,3-Triazol and Benzoxazine Groups in the Main Chain by a Step-Growth Click-Coupling Reaction.'' *J. Polym. Sci. Part A Polym. Chem.*, **46** (7) 2316–2325 (2008)
43. Kiskan, B, Demiray, G, Yagci, Y, ''Thermally Curable Polyvinylchloride via Click Chemistry.'' *J. Polym. Sci. Part A Polym. Chem.*, **46** (11) 3512–3518 (2008)
44. Hariharan, A, Srinivasan, K, Murthy, C, Alagar, M, ''A Novel Imidazole-Core-Based Benzoxazine and Its Blends for High-Performance Applications.'' *Ind. Eng. Chem. Res.*, **56** (33) 9347–9354 (2017)
45. Hariharan, A, Kesava, M, Alagar, M, Dinakaran, K, Subramanian, K, ''Optical, Electrochemical, and Thermal Behavior of Polybenzoxazine Copolymers Incorporated with Tetraphenylimidazole and Diphenylquinoline.'' *Polym. Adv. Technol.*, **29** (1) 355–363 (2018)
46. Selvi, M, Devaraju, S, Vengatesan, MR, Alagar, M, ''Synthesis and Characterization of Heterocyclic Core-Based Polybenzoxazine Matrices.'' *J. Appl. Polym. Sci.*, **136** (9) 47134 (2019)
47. Lin, Z, Liu, Y, Wong, CP, ''Facile Fabrication of Superhydrophobic Octadecylamine-Functionalized Graphite Oxide Film.'' *Langmuir*, **26** (20) 16110–16114 (2010)
48. Zhou, Z, Zhuo, J, Yan, S, Ma, L, ''Design and Synthesis of 3,5-Diaryl-4,5-dihydro-1*H*-pyrazoles as New Tyrosinase Inhibitors.'' *Bioorg. Med. Chem.*, **21** (7) 2156–2162 (2013)
49. Ishida, H, Allen, DJ, ''Physical and Mechanical Characterization of Near-Zero Shrinkage Polybenzoxazines.'' *J. Polym. Sci. Part B Polym. Phys.*, **34** (6) 1019–1030 (1996)
50. Osaki, K, Inoue, T, Uematsu, T, ''Stress Overshoot of Polymer Solutions at High Rates of Shear: Semidilute Polystyrene Solutions With and Without Chain Entanglement.'' *J. Polym. Sci. Part B Polym. Phys.*, **38** (24) 3271–3276 (2000)
51. Vimala, K, Sundarraj, S, Paulpandi, M, Vengatesan, S, Kannan, S, ''Green Synthesized Doxorubicin Loaded Zinc Oxide Nanoparticles Regulates the Bax and Bcl-2 Expression in Breast and Colon Carcinoma.'' *Process. Biochem.*, **49** (1) 160–172 (2014)
52. Agag, T, Arza, CR, Maurer, FHJ, Ishida, H, ''Primary Amine-Functional Benzoxazine Monomers and Their Use for Amide-Containing Monomeric Benzoxazines.'' *Macromolecules*, **43** (6) 2748–2758 (2010)
53. Van Krevelen, DW, *Properties of Polymers: Their Estimation and Correlation with Chemical Structure*. Elsevier, Boca Raton (1976)
54. Hung, HM, Linh, DK, Chinh, NT, Duc, LM, Trung, VQ, ''Improvement of the Corrosion Protection of Polypyrrole Coating for CT3 Mild Steel with 10-Camphorsulfonic Acid

and Molybdate as Inhibitor Dopants.'' *Prog. Org. Coat.*, **131** 407–416 (2019)
55. Koga, GY, Wolf, W, Schulz, R, et al., ''Corrosion and Wear Properties of FeCrMnCoSi HVOF Coatings.'' *Surf. Coat. Technol.*, **357** 993–1003 (2019)
56. Kaur, H, Sharma, J, Jindal, D, Arya, RK, Ahuja, SK, Arya, SB, ''Crosslinked Polymer Doped Binary Coatings for Corrosion Protection.'' *Prog. Org. Coat.*, **125** 32–39 (2018)
57. Morończyk, B, Ura-Bińczyk, E, Kuroda, S, Jaroszewicz, J, Molak, RM, ''Microstructure and Corrosion Resistance of Warm Sprayed Titanium Coatings with Polymer Sealing for Corrosion Protection of AZ91E Magnesium Alloy.'' *Surf. Coat. Technol.*, **363** 142–151 (2019)
58. Sharifi, Z, Pakshir, M, Amini, A, Rafiei, R, ''Hybrid Graphene Oxide Decoration and Water-Based Polymers for Mild Steel Surface Protection in Saline Environment.'' *J. Ind. Eng. Chem.*, **74** 41–54 (2019)
59. Ocón, P, Cristobal, AB, Herrasti, P, Fatas, E, ''Corrosion Performance of Conducting Polymer Coatings Applied on Mild Steel.'' *Corros. Sci.*, **47** 649–662 (2005)
60. Zhou, C, Lu, X, Xin, Z, Liu, J, ''Corrosion Resistance of Novel Silane-Functional Polybenzoxazine Coating on Steel.'' *Corros. Sci.*, **70** 145–151 (2013)
61. Nayak, SR, Mohana, KNS, ''Corrosion Protection Performance of Functionalized Graphene Oxide Nanocomposite Coating on Mild Steel.'' *Surf. Interfaces*, **11** 63–73 (2018)
62. Zheng, H, Guo, M, Shao, Y, Wang, Y, Liu, B, Meng, G, ''Graphene Oxide–Poly(urea–Formaldehyde) Composites for Corrosion Protection of Mild Steel.'' *Corros. Sci.*, **1–12** 139 (2018)
63. Hao, YS, Liu, FC, Han, EH, Anjum, S, Xu, GB, ''The Mechanism of Inhibition by Zinc Phosphate in an Epoxy Coating.'' *Corros. Sci.*, **69** 77–86 (2013)
64. Benea, L, Mardare, L, Simionescu, N, ''Anticorrosion Performances of Modified Polymeric Coatings on E32 Naval Steel in Sea Water.'' *Prog. Org. Coat.*, **123** 120–127 (2018)
65. Zhang, Y, Shao, Y, Liu, X, et al., ''A Study on Corrosion Protection of Different Polyaniline Coatings for Mild Steel.'' *Prog. Org. Coat.*, **111** 240–247 (2017)